Kondo resonances and Fano antiresonances in transport through quantum dots

M. E. Torio,[1] K. Hallberg,[2] A. H. Ceccatto,[1] and C. R. Proetto[2]
[1]*Instituto de Física de Rosario, CONICET-UNR, Boulevard 27 de Febrero 210bis, 2000 Rosario, Argentina*
[2]*Centro Atómico Bariloche and Instituto Balseiro, Comisión Nacional de Energía Atómica, 8400 Bariloche, Argentina*
(Received 10 August 2001; published 28 January 2002)

The transmission of electrons through a noninteracting tight-binding chain with an interacting *side* quantum dot (QD) is analyzed. When the Kondo effect develops at the dot the conductance presents a wide minimum, reaching zero at the unitary limit. This result is compared to the opposite behavior found in an embedded QD. Application of a magnetic field destroys the Kondo effect and the conductance shows pairs of dips separated by the charging energy *U*. The results are discussed in terms of Fano antiresonances and explain qualitatively recent experimental results.

DOI: 10.1103/PhysRevB.65.085302 PACS number(s): 73.63.−b, 72.15.Qm

Semiconductor quantum dots (QD) are small droplets of electrons, confined in the three spatial directions. Energy and charge quantization results from this confinement. As both features are shared with real atomic systems, from the very beginning, an extremely useful analogy has been exploited between ''real'' and ''artificial'' atomic systems. This analogy received strong support through an experimental breakthrough where the Kondo effect in quantum dots was unambiguously measured.[1,2] Historically, the Kondo effect was introduced about 40 years ago to explain the resistivity minimum for decreasing temperatures observed in metallic matrices with a minute fraction of magnetic impurities.[3] According to the detailed microscopic theory, when the temperature T decreases below the Kondo temperature T_K, the localized magnetic impurity starts to interact strongly with the surrounding electronic cloud, which finally results in a singlet many-body ground state, reaching its maximum strength at $T=0$.[4] The minimum in the resistivity results from the fact that, as the temperature is lowered, the scattering with phonons decreases down to the Kondo temperature at which the scattering with localized impurities becomes important as the Kondo effect is operative. It is important to emphasize that in this case, the so-called traditional Kondo effect, magnetic impurities act as scattering centers, *increasing* the sample resistivity.

The opposite behavior is found in the Kondo effect in quantum dots. The situation considered almost without exception both theoretically and experimentally, consists of a quantum dot connected to two leads in such a way that electrons transmitted from one electrode to the other should necessarily pass through the quantum dot (a *substitutional* dot). As theoretical calculations predicted,[5,6] in this configuration the conductance *increases* when the temperature decreases and the Kondo effect sets in, essentially due to a resonant transmission through the so-called Kondo resonance, which appears in the local density of states at the dot site at the Fermi level. In this situation, at $T=0$, the conductance should take the limiting value $2e^2/h$, corresponding to the unitary limit of a one-dimensional perfect transmission channel.[7]

The aim of this work is to analyze an alternative configuration of a *side-coupled* quantum dot, attached to a perfect quantum wire. In this case, the quantum dot acts as a scattering center for transmission through the chain, in close analogy with the traditional Kondo effect. We have found that when the dot provides a resonant energy for scattering, the conductance has a sharp decrease, reminiscent of the Fano antiresonances observed in scanning-tunneling-microscope experiments for magnetic atoms on a metallic substrate.[8] A similar problem has been discussed both by Kang *et al.*[9] and by Bulka and Stefański.[10] However, in Ref. 9 the authors use the approximate slave-boson mean-field theory to describe the Kondo regime in the limit $U\to\infty$, while in Ref. 10 the configuration considered is different from ours. In this paper we show that by using a very precise numerical technique appropriate for this system, we can incorporate the effects of a realistic value of the charging energy *U*. This allows us to obtain the features observed experimentally, e.g., the double-dip structures of Fig. 3, which give rise to the diamond-shaped features in differential conductance experiments.[11]

The models employed in the calculation are schematically shown in Fig. 1. Case (a), corresponding to the *substitutional* dot situation, consists of two semi-infinite noninteracting tight-binding chains connected to a central site (the dot). Case (b), corresponding to the *side* dot, consists of a quan-

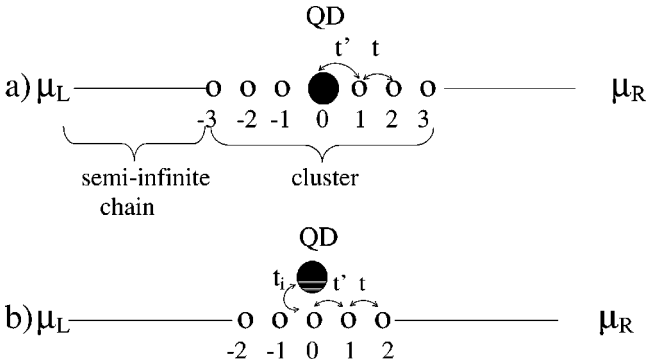

FIG. 1. Schematic representation of our models: (a) *substitutional* dot configuration; (b) *side* dot configuration. Small open circles represent cluster noninteracting sites, big full circles represent the dot site. The cluster includes the dot and a few noninteracting sites. Left and right full lines represent the noninteracting tight-binding semi-infinite chains with their respective chemical potentials μ_L and μ_R.

 ©2002 The American Physical Society

tum wire coupled sideways to a QD. The dot is modeled as an Anderson impurity. The Hamiltonian reads

$$\mathcal{H}=\mathcal{H}_0+\mathcal{H}_{int}, \tag{1}$$

where $\mathcal{H}_0$ is the Hamiltonian of two semi-infinite chains

$$\mathcal{H}_0=-\sum_{j\leqslant -1,\sigma} t_j(c^\dagger_{j\sigma}c_{j+1\sigma}+\text{H.c.}) - \sum_{j\geqslant 0,\sigma} t_j(c^\dagger_{j\sigma}c_{j+1\sigma}+\text{H.c.}), \tag{2a}$$

and $\mathcal{H}_{int}$ can be written as

$$\mathcal{H}^a_{int}=\sum_\sigma \varepsilon_\sigma c^\dagger_{0\sigma}c_{0\sigma}+\frac{U}{2}n_{0\sigma}n_{0\bar{\sigma}} \tag{2b}$$

for the *substitutional* dot configuration, while

$$\mathcal{H}^b_{int}=\sum_\sigma -t_i(c^\dagger_{0\sigma}c_\sigma+\text{H.c.})+\varepsilon_\sigma c^\dagger_\sigma c_\sigma+\frac{U}{2}n_\sigma n_{\bar{\sigma}} \tag{2c}$$

for the *side* dot configuration. In the equations above, $t_j=t$ for $j\leqslant -2$, $j\geqslant 1$, while $t_{-1}=t_0=t'$, $n_{0\sigma}=c^\dagger_{0\sigma}c_{0\sigma}$, $n_\sigma=c^\dagger_\sigma c_\sigma$, and $U>0$. As we are also interested in the behavior in a magnetic field H, we consider the local energies as $\varepsilon_\uparrow=\varepsilon_0+\Delta\varepsilon/2$, $\varepsilon_\downarrow=\varepsilon_0-\Delta\varepsilon/2$, with $\Delta\varepsilon=g\mu_B H$ the Zeeman splitting of the localized orbital, i.e., the principal magnetic field effect is to shift the local QD levels.[12] It is interesting to point out that both models could be mapped to a single semi-infinite chain, with the dot sitting at the free end, and the remaining sites corresponding to the even basis states that couples to the dot.[13] Both models become exactly equivalent from the point of view of their equilibrium properties,[14] if the hoppings are related as follows: $t_i=\sqrt{2}t'=t$. However, as we show below, the transport properties of both models are completely different.

For the analysis of our transport results, we have used the following equation for the magnetic-field-dependent conductance,[15] in the linear-response regime ($\mu_L\to 0^+$ and $\mu_R\to 0^-$):

$$G(H)=\frac{e^2}{h}\frac{2\pi t'^2}{t}\sum_\sigma \rho_\sigma(\omega=0), \tag{3}$$

where $\rho_\sigma(\omega)$ is the local density of states (per spin) at site 0 evaluated at the Fermi energy $\omega=0$.

To obtain the density of states $\rho_\sigma(\omega=0)$ we use a combined method. In the first place we consider an open finite cluster of N sites [$N=7$ for case (a) and 6 for case (b)] which includes the impurity. This is diagonalized using the exact-diagonalization Lanczos technique.[16] We then proceed to embed the cluster in an external reservoir of electrons, which fixes the Fermi level of the system, attaching two semi-infinite leads to its right and left.[17] This is done by calculating the one-particle Green's function $\hat{G}$ of the whole system within the chain approximation of a cumulant expansion[18] for the dressed propagators. This leads to the Dyson equation $\hat{G}=\hat{G}\hat{g}+\hat{T}\hat{G}$, where $\hat{g}$ is the cluster Green's function obtained by the Lanczos method. Following Ref. 17, the charge fluctuation inside the cluster is taken into account by writing $\hat{g}$ as a combination of n and $n+1$ particles with weights $1-p$ and p respectively, $\hat{g}=(1-p)\hat{g}_n+p\hat{g}_{n+1}$. The total charges of the cluster and p are calculated by solving self-consistently the equations

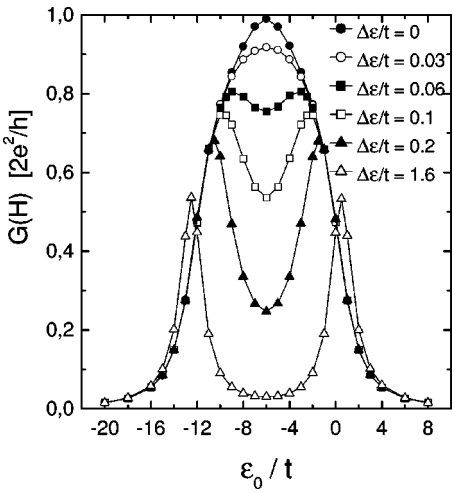

FIG. 2. Conductance (in units of $2e^2/h$) for the *substitutional* dot configuration, as a function of the impurity level position and for several values of the magnetic field ($t'/t=1/\sqrt{2}$ and $U/t=12$).

$$Q_c=n(1-p)+(n+1)p, \tag{4}$$

$$Q_c=-\frac{1}{\pi}\int_{-\infty}^{\epsilon_F}\sum_i \text{Im}\ G_{ii}(\omega)d\omega, \tag{5}$$

where i runs on the cluster sites. Once convergence is reached, the density of states is obtained from $\hat{G}$. It is important to stress that this method is reliable only if t' is large enough, so that the Kondo cloud is about the size of the cluster (for the parameters used here we estimate a Kondo correlation length of about 10 lattice sites). Moreover, the fact that the conductance reaches the unitary limit for the symmetric case provides an important test of the validity of the method (see Fig. 2).

In order to compare both geometrical realizations we present in Fig. 2 the conductance for the *substitutional* QD [Fig. 1(a)]. As discussed above, at zero temperature and magnetic field, the Kondo resonance, which develops right at the Fermi level, greatly enhances the transmission when the average dot occupancy is close to (but less than) 1, i.e., in the Kondo regime. For the symmetric situation $\varepsilon_0=-U/2$, the transmission is perfect and the conductance reaches the unitary limit $G(0)=2e^2/h$.[19] This is a nontrivial check from the numerical point of view, and proves that our finite-system approach produces a Kondo peak with the exact spectral weight at the Fermi energy. Within our approach, the Coulomb-blockade peaks become discernible through the application of a magnetic field. As seen in Fig. 2, with increasing magnetic field, spin fluctuations at the impurity site are progressively quenched, and the associated enhancement of the conductance turns into a valley flanked by two Coulomb-

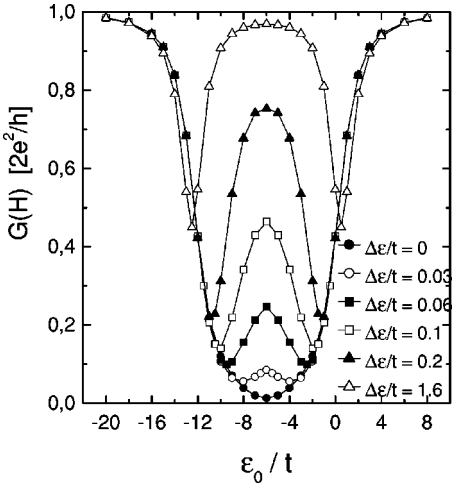

FIG. 3. Same as Fig. 2 for the *side* dot configuration ($t_i/t=1$).

blockade peaks roughly separated by U. On the other side, the Coulomb-blockade peaks are rather insensitive to magnetic-field effects.

The equivalent to the traditional Kondo effect, corresponding to the geometrical arrangement of Fig. 1(b), is shown in Fig. 3. In this configuration, the conductance reaches the unitary limit either when the dot is fully occupied ($\varepsilon_0+U<0$) or empty ($\varepsilon_0>0$). In both cases, the *side* dot weakly perturbs the transmission along the tight-binding chain, as the possible scattering processes disappear. On the other side, the conductance becomes progressively blocked as the *side* dot enters in the Kondo regime, reaching the antiunitary limit $G(0)=0$ exactly at the *side* dot symmetric configuration $\varepsilon_0=-U/2$. In other words, even though the noninteracting central site provides, in principle, a channel for transmission, through its coupling to the *side* dot it becomes a perfectly reflecting barrier.

The results for the total ($\rho_\uparrow+\rho_\downarrow$) local density of states (DOS) shown in Fig. 4 provides a nice qualitative explanation of the linear conductance results in both geometrical arrangements. Figures 4(a) and 4(b) correspond to the local DOS at sites 0 and at the dot respectively, both for the *side* dot configuration. Starting with Fig. 4(b), a well-defined Kondo resonance is discernible around the Fermi level in the absence of a magnetic field. The exact (unitary) zero-field result $\rho_{imp}(\omega=0)=t/(\pi t'2)=2/(\pi t)\simeq 0.64$ (for $t=1$ and $t'/t=1/\sqrt{2}$) is recovered from our numerical approach, as discussed above.

For these parameters, the local DOS at the impurity site in the *side* dot configuration is equivalent to the local DOS at the impurity in the *substitutional* dot configuration, and gives rise to the unitary limit $G(0)=2e^2/h$ discussed above. From the full width of the zero-field impurity DOS at half-maximum, we estimate $k_BT_K/t\simeq 0.3$ for these parameters; note that this estimate agrees qualitatively with the magnetic-field values for which the Kondo effect is destroyed (see Fig. 3). In the presence of a magnetic field, the Kondo resonance splits into two peaks, generating a local minimum between them. As the conductance in the *substitutional* dot configuration is proportional to the dot DOS at the Fermi level, this

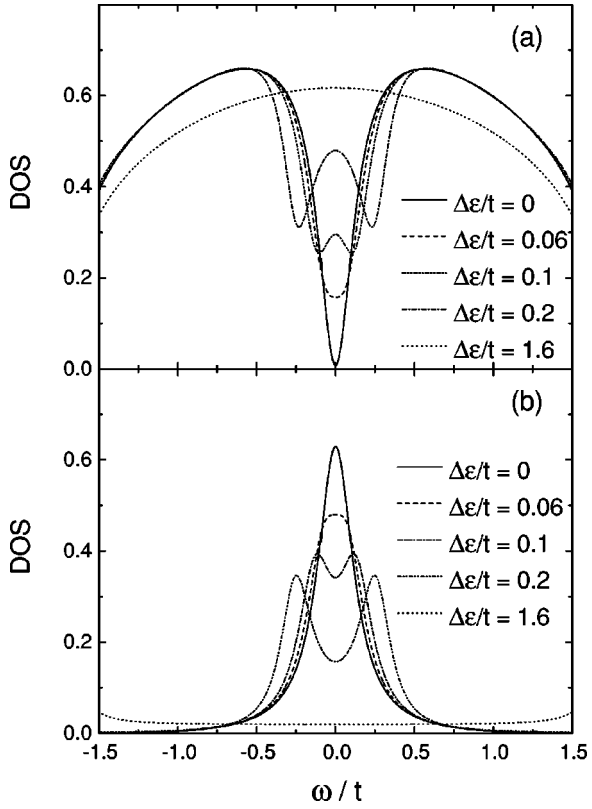

FIG. 4. Local density of states for the *side* dot configuration corresponding to the symmetric situation $\varepsilon_0=-U/2$ for different values of magnetic field: (a) at the noninteracting site 0 of the tight-binding chain; (b) at the QD site (same parameters as in Fig. 3).

explains the abrupt decrease of $G(H)$ with increasing H at the middle of the Kondo valley shown in Fig. 2.

Coming back to the *side* dot, the most noticeable features of Fig. 4(a), corresponding to the DOS at site 0 of the chain, are the profound dips it exhibits around the Fermi level; a pseudogap appears for $H=0$ at the symmetric situation $\varepsilon_0=-U/2$ exactly at the Fermi level. The existence of this pseudogap explains the conductance minimum of Fig. 3 at $\varepsilon_0=-U/2$. In the presence of a magnetic field, the dip weakens and accordingly the conductance starts to increase. After a certain threshold field, the DOS develops a double-well shape around the Fermi level; the distance between the two well minima is about $2\Delta\varepsilon$.[20] If the magnetic field is strong enough ($\Delta\varepsilon/k_BT_K\gg 1$), the Kondo effect is destroyed, the associated coupling between the quantum wire and the side dot essentially vanishes, and the DOS at site 0 recovers the semielliptical shape corresponding to the noninteracting chain with $t=\sqrt{2}t'=t_i$.

Conceptually, the simplest way to understand these transport features is using the framework developed by Fano 40 years ago.[21] He analyzed the properties of a system consisting of a continuous spectrum degenerated with a discrete level, both noninteracting. Under these conditions, a dip develops in the density of states of the continuous spectrum, as a result of its interaction with the discrete level. In our case, the continuous spectrum is provided by the tight-binding

chain, while the role of the discrete level is played by the Kondo peak at the DOS of the *side* dot. The Kondo peak in the local DOS at the *side* dot is produced at the expense of a decrease of the local DOS at the neighboring site 0. As the Kondo effect is destroyed by the magnetic field, its associated many-body Fano antiresonance[22] weakens. An interesting feature of our calculation is the evolution of $G(H)$ for increasing H: as the Kondo effect is destroyed, the wide minimum develops a high-conductance region around the Fermi level. At high fields, the conductance shows two dips, roughly separated by U. These two dips are again quite natural in the Fano framework: the *side* dot DOS, besides the Kondo peak, has two single-particle resonances at ε_0 and ε_0+U [not shown in Fig. 4(b)]. They give rise to the Coulomb-blockade peaks in the *substitutional* dot configuration (see Fig. 2 at a high-magnetic-field situation). However, in the *side* dot configuration, they play the role of two discrete levels, which also produce a Fano antiresonance when these levels coincide with the Fermi energy ($\varepsilon_0=0$ and $\varepsilon_0+U=0$): the result is now two Coulomb *dips* instead two Coulomb-blockade *peaks*. In view of this analysis, it is clear that the wide valley of Fig. 3 results from the superposition of two effects: one due to the Kondo effect around $\varepsilon_0=-U/2$, and the other due to charge fluctuations between the dot and the leads around $\varepsilon_0=0$ and $\varepsilon_0+U=0$.

We believe that our calculations shed light on recent experiments by Göres *et al.*[11] Using the same samples as in Ref. 1, and changing the transmission of the left and right tunnel barriers that connect the dot to the conducting leads, they perform conductance measurements in the Fano regime (strong coupling leads dot), the Kondo regime (intermediate coupling), and the Coulomb-blockade regime (weak coupling leads-dot). The main results concern the Fano regime, where the conductance shows asymmetric Fano dips on top of a slowly varying background. Some features of the dips are reminiscent of the Kondo effect, as the temperature dependence of their amplitude (Fig. 4 in Ref. 11), and others of the Coulomb-blockade effect, as the typical diamond-shaped structure in differential conductance measurements (Fig. 5 in Ref. 11). Both features are easily explained by our results. While our calculation is valid for $T=0$, it seems reasonable to expect similar qualitative behavior by increasing the temperature at $H=0$: a wide valley for $T<T_K$ and two narrow dips separated by U for $T>T_K$. Accordingly, one can expect a strong dependence of the dip amplitude on temperature, decreasing for increasing temperature. Besides, the behavior of dips in differential conductance measurements should be completely analogous to the related Coulomb-blockade peaks, leading to diamond-shaped structures for the dips. While the geometry of the experiment by Göres *et al.* corresponds to our substitutional dot configuration, their results in the Fano regime could be interpreted as due to the presence of two conducting channels through the dot: one (nonresonant) channel strongly coupled to the leads, and a second (resonant) channel weakly coupled to the leads, with an additional coupling between both channels. This *two-level* substitutional model directly maps on our *one-level* side dot configuration, with the site 0 of the chain playing the role of the nonresonant channel and the QD corresponding to the weakly coupled (actually, zero-coupled) resonant channel. However, it should be mentioned that in addition to rather symmetric dips, Göres *et al.* found also very asymmetric dips in the strongly coupled regime, as shown in their Fig. 2(a). These asymmetric dips are beyond the scope of our model, as they will arise by giving a finite amplitude for (direct) transmission through the side dot, this amplitude being zero in our model (see also Ref. 23). Our results also shed light on the somehow related problem of the persistent current in a mesoscopic ring with a *side* dot.[24,25] The results remain controversial on this issue, as Ref. 24 found a detrimental effect of the *side* dot on the persistent current when the Kondo effect is operative. An opposite result was found in Ref. 25, with the ring exhibiting a perfect (unitary) persistent current in the Kondo regime. Our results for the open configuration of the present work provide naturally strong support to the detrimental effect found by Affleck and Simon.[24]

The authors are grateful to C. A. Balseiro for several illuminating discussions. The authors acknowledge support from CONICET. This work was supported partially by Grants Nos. PIP 0473/98 (CONICET), PICT97 03-00121-02152 (ANPCyT), and PICT 03-03833 (ANPCyT).

[1] D. Goldhaber-Gordon *et al.*, Nature (London) **391**, 156 (1998).
[2] S. M. Cronenwet, T. H. Oosterkamp, and L. P. Kouwenhoven, Science **281**, 540 (1998).
[3] J. Kondo, Solid State Phys. **23**, 183 (1969).
[4] A. C. Hewson, *The Kondo Problem to Heavy Fermions* (Cambridge University Press, Cambridge, U.K. 1993).
[5] L. I. Glazman and M. E. Raikh, JETP Lett. **47**, 452 (1988).
[6] T. K. Ng and P. A. Lee, Phys. Rev. Lett. **61**, 1768 (1988).
[7] W. G. van der Wiel, S. De Franceschi, T. Fujisawa, J. M. Elzerman, S. Tarucha, and L. P. Kouwenhoven, Science **289**, 2105 (2000).
[8] V. Madhavan, W. Chen, T. Jamneala, M. F. Crommie, and N. S. Wingreen, Science **280**, 567 (1998); J. Li, W.-D. Schneider, R. Berndt, and B. Delley, Phys. Rev. Lett. **80**, 2893 (1998).
[9] K. Kang, S. Y. Cho, J. J. Kim, and S. C. Shin, Phys. Rev. B **63**, 113304 (2001).
[10] B. R. Bulka and P. Stefański, Phys. Rev. Lett. **86**, 5128 (2001).
[11] J. Göres, D. Goldhaber-Gordon, S. Heemeyer, M. A. Kastner, H. Shtrikman, D. Mahalu, and U. Meirav, Phys. Rev. B **62**, 2188 (2000).
[12] Y. Meir, N. S. Wingreen, and P. A. Lee, Phys. Rev. Lett. **70**, 2601 (1993).
[13] J. Simonin (private communication).
[14] P. Schlottmann, Phys. Rev. B **17**, 2497 (1978).
[15] Y. Meir and N. S. Wingreen, Phys. Rev. Lett. **68**, 2512 (1992).
[16] E. Dagotto and A. Moreo, Phys. Rev. D **31**, 865 (1985); E. Gagliano, E. Dagotto, A. Moreo, and F. Alcaraz, Phys. Rev. B **34**, 1677 (1986).

[17] V. Ferrari, G. Chiappe, E. V. Anda, and M. A. Davidovich, Phys. Rev. Lett. **82**, 5088 (1999).
[18] C. Caroli, R. Combescot, P. Nozieres, and D. Saint-James, J. Phys. C **4**, 916 (1971); W. Metzner, Phys. Rev. B **43**, 8549 (1991).
[19] It is interesting to note that only recently this unitary limit has been experimentally achieved in Ref. 7.
[20] A similar result has been predicted in Ref. 12 and measured in Refs. 1 and 2 for the *substitutional* case.
[21] U. Fano, Phys. Rev. **124**, 1866 (1961).
[22] J. L. D'Amato, H. M. Pastawski, and J. F. Weisz, Phys. Rev. B **39**, 3554 (1989).
[23] W. Hofstetter, J. Köning, and H. Schoeller, Phys. Rev. Lett. **87**, 156803 (2001).
[24] I. Affleck and P. Simon, Phys. Rev. Lett. **86**, 2854 (2001).
[25] H.-P. Eckle, H. Johannesson, and C. A. Sttaford, Phys. Rev. Lett. **87**, 016602 (2001).